Journal of Marine Systems 139 (2014) 261–275

Contents lists available at ScienceDirect

Journal of Marine Systems

journal homepage: www.elsevier.com/locate/jmarsys

Modelling dinoflagellates as an approach to the seasonal forecasting of bioluminescence in the North Atlantic

Charlotte L.J. Marcinko [a,b,*], Adrian P. Martin [b], John T. Allen [c]

[a] Ocean and Earth Sciences, University of Southampton, University of Southampton Waterfront Campus, Southampton SO14 3ZH, UK
[b] National Oceanography Centre, European Way, Southampton SO14 3ZH, UK
[c] School of Earth and Environmental Sciences, University of Portsmouth, Burnaby Building, Burnaby Road, Portsmouth, Hampshire PO1 3QL, UK

ARTICLE INFO

Article history:
Received 30 January 2014
Received in revised form 19 May 2014
Accepted 30 June 2014
Available online 6 July 2014

Keywords:
Bioluminescence
Dinoflagellate
Ecosystem
Model
Forecast
Atlantic

ABSTRACT

Bioluminescence within ocean surface waters is of significant interest because it can enhance the study of subsurface movement and organisms. Little is known about how bioluminescence potential (BPOT) varies spatially and temporally in the open ocean. However, light emitted from dinoflagellates often dominates the stimulated bioluminescence field. As a first step towards forecasting surface ocean bioluminescence in the open ocean, a simple ecological model is developed which simulates seasonal changes in dinoflagellate abundance. How forecasting seasonal changes in BPOT may be achieved through combining such a model with relationships derived from observations is discussed and an example is given. The study illustrates a potential new approach to forecasting BPOT through explicitly modelling the population dynamics of a prolific bioluminescent phylum. The model developed here offers a promising platform for the future operational forecasting of the broad temporal changes in bioluminescence within the North Atlantic. Such forecasting of seasonal patterns could provide valuable information for the targeting of scientific field campaigns.

1. Introduction

Many marine organisms are capable of producing visible light, known as bioluminescence (Haddock et al., 2010; Widder, 2010). Bioluminescence is ubiquitous throughout the world's oceans and in certain conditions, highly visible displays of blue light (474–476 nm) can be stimulated via hydrodynamic stresses induced by surface and subsurface movement (e.g. Fig. 1). In situ measurement of bioluminescence offers a number of applications for assessing the wider ocean environment (Herring and Widder, 2001; Moline et al., 2007). This includes the study of subsurface physical dynamics such as internal waves (Kushnir et al., 1997) and the evaluation of fish stocks using intensified cameras at night to identify fish schools (Churnside et al., 2012; Squire and Krumboltz, 1981). Thus, the ability to forecast its occurrence in surface waters and to assess when the illumination of near-surface motion may occur is of significant interest.

Previous attempts to model bioluminescence have focused upon simulating its distribution over relatively large spatial scales (1000–2000 km) or forecasting changes in its spatial distribution on time scales of the order of days (Ondercin et al., 1995; Shulman et al., 2003, 2011, 2012). Models have been based upon empirical relationships between bioluminescence and other biogeochemical environmental variables such as chlorophyll (Ondercin et al, 1995) or the advancement of the bioluminescence field through physical advective and diffusive processes (Shulman et al, 2003, 2011). These models have had limited success in simulating the distribution of the bioluminescence field (reviewed in Marcinko et al., 2013a). The lack of success indicates that the distribution of bioluminescent organisms will not always coincide with that of the phytoplankton dominating the chlorophyll signal or be correlated with physical properties. The ecological and behavioural dynamics of the bioluminescent organisms themselves must be considered for the forecasting of bioluminescence to be improved (Shulman et al., 2012).

Bathyphotometer measurements of flow stimulated bioluminescence provide a measure of the bioluminescent potential (BPOT) of a volume of water. Field measurements indicate that dinoflagellates are a major source of bioluminescence and that their light emissions often dominate the BPOT measured in the surface ocean (Batchelder and Swift, 1989; Lapota et al., 1992; Latz and Rohr, 2005; Neilson et al., 1995; Seliger et al., 1962). Although only a small proportion of dinoflagellates are known to be bioluminescent (around 70 out of approximately 1500 species) a number of studies have found positive associations between BPOT and total dinoflagellate cell abundance (i.e.

* Corresponding author. Tel.: +44 2380 596338.
E-mail addresses: c.marcinko@noc.ac.uk (C.L.J. Marcinko), adrian.martin@noc.ac.uk (A.P. Martin), john.allen@port.ac.uk (J.T. Allen).

http://dx.doi.org/10.1016/j.jmarsys.2014.06.014

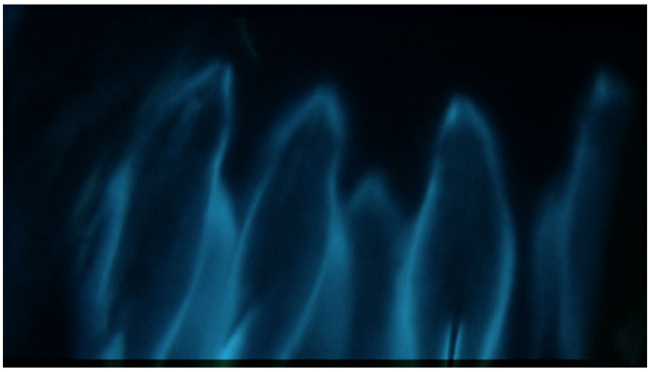

Fig. 1. Dolphins illuminated by dinoflagellate bioluminescence at night as they swim through the ocean (provided by Ammonite Films).

bioluminescent plus non-bioluminescent species). For instance, within the Mediterranean and Black Seas a compilation of over 3500 bioluminescent measurements and 1000 phytoplankton samples between 1970 and 1995 showed extremely strong positive relationships ($r^2 = 0.95$ to 0.98; $p < .05$) between BPOT and dinoflagellate cell abundance (Tokarev et al., 1999). Similarly, positive correlations ($r = 0.86–0.93$; $p < .05$) have been found in the mouth of the Vestfjord, Norway (Lapota et al., 1989) and the MLML programme, which conducted several cruises in the Irminger Sea between 1989 and 1991 (Marra, 1995), found dinoflagellates were responsible for >90% of BPOT throughout spring, summer and autumn (Swift et al., 1995).

The findings of the studies described above suggest that temporal changes in dinoflagellate abundance can be used as a proxy for seasonal variations in BPOT. Therefore, explicitly modelling dinoflagellate population dynamics could provide a feasible approach to operational forecasting of BPOT, where 'operational forecasting' is the term widely used to describe the prediction of a specific event using a practical means. This approach is particularly promising in non-coastal regions where bioluminescent populations are often mixed and modelling individual species is not possible. A successful dynamical model incorporating a 'dinoflagellate' functional group will potentially have the capability to reproduce much of the seasonal and large scale spatial variation of the bioluminescence field (Marcinko et al., 2013a).

The modelling of dinoflagellates has largely focused on Harmful Algal Bloom (HAB) species in specific coastal areas (Anderson, 1998; Franks, 1997; Montagnes et al., 2008; Olascoaga et al., 2008; Walsh et al., 2001) or on dinoflagellates as a functional type in regional coastal waters (Cugier et al., 2005; Vanhoutte-Brunier et al., 2008). There have been relatively few attempts to model dinoflagellates within the open ocean as they are infrequently regarded as a key species of interest in the basin and global scale models that this environment spans. Whilst over the past decade understanding the factors controlling populations of other phytoplankton groups, such as diatoms, has advanced substantially, modelling of dinoflagellates, particularly as a mixed population away from coastal areas, is still for the most part in its infancy (Hood et al., 2006). Only in the past decade have larger scale models begun to break phytoplankton down into its constituent functional groups (e.g. Follows et al., 2007; Le Quere et al., 2005; Merico et al., 2004; Vichi et al., 2007). However, dinoflagellates still tend to be overlooked within models as they are often considered less important when compared to other phytoplankton groups in terms of their role in carbon sequestration, remineralisation, nitrification and calcification. Dinoflagellates also, unlike phytoplankton groups such as diatoms, do not have a well-characterised defining biogeochemical characteristic, such as silicate limitation, that can be directly modelled and used to define them as a functional type.

The Luminescence And Marine Plankton (LAMP) project aimed to determine the predictability of bioluminescence through investigating dinoflagellates—the planktonic functional group responsible for the majority of BPOT stimulated in the surface oceans. As part of the LAMP project, this study describes the development, parameterisation and testing of an ecosystem model which simulates broad temporal changes in dinoflagellate abundance within an open ocean region of the North-east Atlantic. The study aims to illustrate how such a model could provide a platform for the future operational forecasting of surface BPOT within the North Atlantic. We take a purposefully simplistic modelling approach combined with the limited available bioluminescence data to conceptualise how the forecasting of surface BPOT could be advanced in the future.

2. Study area

The model aims to simulate a typical annual cycle (for the years between 2001 and 2007) within the waters surrounding the Porcupine Abyssal Plain sustained observatory; the black box shown in Fig. 2 based on the standard area E5 of the Continuous Plankton Recorder Survey (CPR). This region is characterised by a large spring phytoplankton bloom (Ducklow and Harris, 1993) dominated by diatoms (Barlow et al., 1993; Lochte et al., 1993). The spring bloom is followed by the proliferation of other organisms (Barlow et al., 1993; Lochte et al., 1993) and observations show that dinoflagellates contribute significantly to the post bloom summer phytoplankton population (Dodge, 1993; Leterme et al., 2005; Smythe-Wright et al., 2010). The study region was chosen to coincide with previous LAMP experiments (Marcinko et al., 2013b) and because of the availability of data required for model optimisation and assessment.

3. Model description

A schematic of the model including the flows between state variables is shown in Fig. 3. The model contains five components representing the interactions between nutrients, phytoplankton and zooplankton. The biological ecosystem is assumed to be homogenously distributed within an upper mixed layer overlying a deep abiotic layer. Organisms are not modelled in the deeper layer as the study is focused upon interactions within the surface waters. The system is composed of two phytoplankton types, diatoms (P_1) and dinoflagellates (P_2), two nutrients, nitrate (N) and silicate (Si), and one predator type, metazoan zooplankton (Z).

The model provides a simple structure that captures the primary interactions of the ecosystem. Diatoms are included in the model, along with dinoflagellates, because they are known to dominate the spring bloom (Barlow et al., 1993; Lochte et al., 1993) and their depletion of surface water nutrients can have a strong effect on phytoplankton succession. Other phytoplankton groups are not explicitly included within the model primarily due to the lack of data available to constrain associated model parameters. Differences in the dynamics between phytoplankton groups in the model are primarily set through differences in parameter values, which are based on experimental results from species within the respective phytoplankton groups. In addition to these differences in parameters defining key processes such as growth and mortality, dinoflagellates differ from diatoms in the model in terms of sinking. Modelled diatoms sink from the mixed layer and dinoflagellates do not. This difference accounts for many dinoflagellates being motile and within the model their ability to maintain their position within the sun-lit mixed layer provides them with an advantage that promotes growth.

Nitrogen is used as the model currency. A fixed N:Si ratio of 1.0666 (Brzezinski, 1985) is assumed. Similarly a C:N ratio of 6.6250, based on the widely used "Redfield" ratio (Redfield, 1934), and a constant Chl:C ratio of 0.0141, a value corresponding to the midpoint of the range suggested by Behrenfeld et al. (2005) for the north-east Atlantic are assumed. Model equations are set out in Appendix A and a full list of model parameters is given in Table 1.

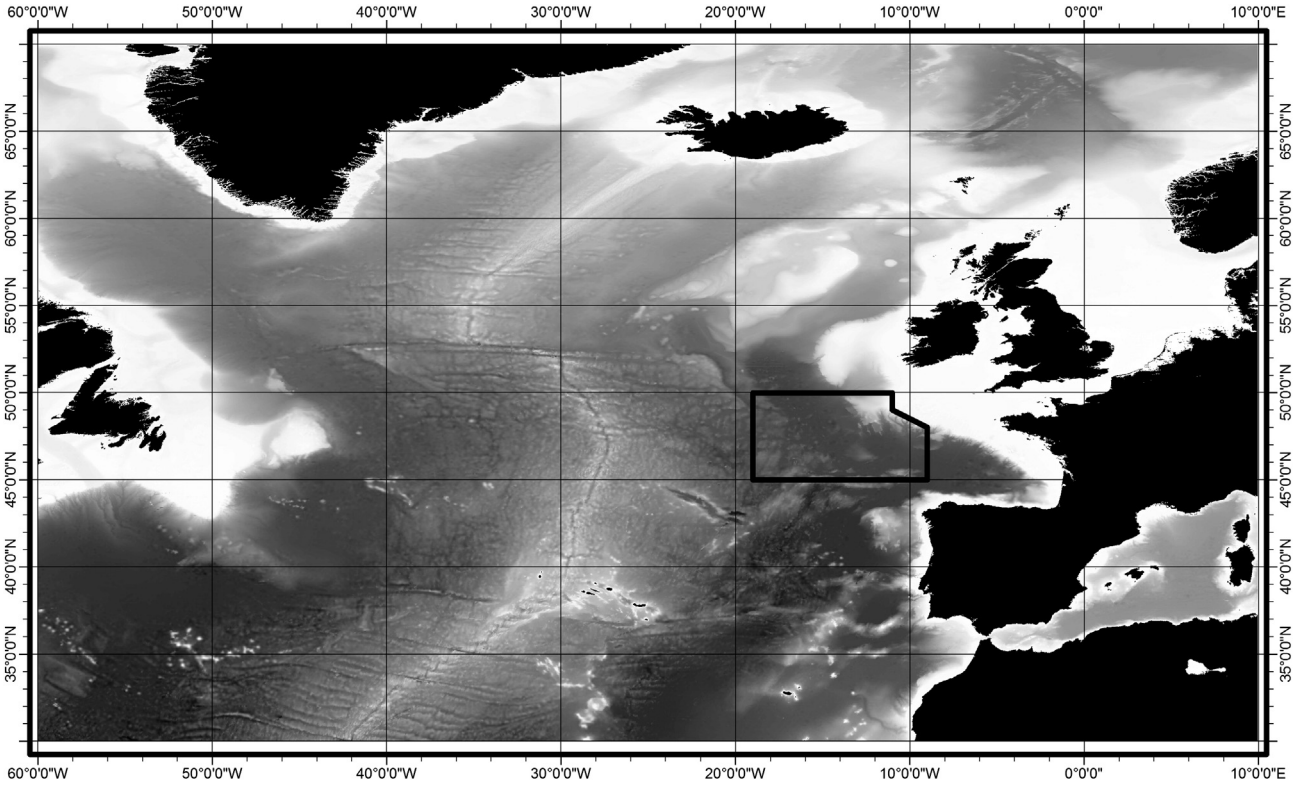

Fig. 2. Study site surrounding the Porcupine Abyssal Plain; based on standard area E5 of the Continuous Plankton Recorder (CPR) survey.

Physical dynamics controlling the mixed layer depth were not explicitly modelled and no horizontal affects, such as advection, were considered. Observational data have been used to define changes in mixed layer depth (MLD), photosynthetically active radiation (PAR) and nutrient concentrations directly below the mixed layer as a function of time (days), and to drive seasonal changes in the ecosystem.

The purpose of this study is to develop a model that can be used a first step towards operationally forecasting (i.e. prediction via practical means) BPOT. The zero-dimensional model presented is chosen primarily because it is simple enough to be well constrained by the available data yet complex enough to simulate the variable of interest (dinoflagellate biomass) required for predicting temporal variation in BPOT. Knowledge that a process exists does not mean that it has to be included in a model to capture first order features of a system. Such an approach can result in a model that is more complicated than necessary (Ward et al., 2013). In the development of all ecosystem models it is necessary to make simplifying assumptions and strike a fine balance between capturing the characteristics of the system that are dynamically

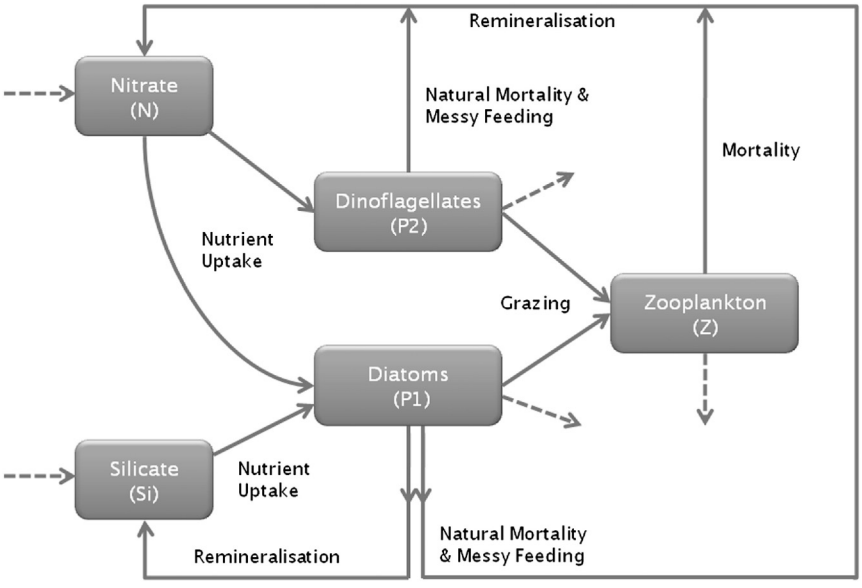

Fig. 3. Model schematic stating major coupling processes between state variables. Solid arrows indicate flows of nitrogen between model components within the mixed layer. Dashed arrows indicate input and output from the mixed layer.

Table 1
List of parameters used in model containing dinoflagellates for the waters surrounding the Porcupine Abyssal Plain for a typical year within the period 2001 to 2007.

Parameter	Symbol	Unit
Phytoplankton		
Maximum growth rate P_1	μ_1	day^{-1}
Maximum growth rate P_2	μ_2	day^{-1}
Nitrate half saturation constant P_1	k_{N1}	mmol m^{-3}
Nitrate half saturation constant P_2	k_{N2}	mmol m^{-3}
Silicate half saturation constant P_1	k_{Si}	mmol m^{-3}
Initial P–I Slope P_1	α_1	$(W\ m^{-2})^{-1}\ day^{-1}$
Initial P–I Slope P_2	α_2	$(W\ m^{-2})^{-1}\ day^{-1}$
Sinking rate P_1	V_{diatom}	m day^{-1}
Phytoplankton maximum natural mortality rate	m_p	day^{-1}
Phytoplankton mortality half saturation constant	k_{mp}	mmol m^{-3}
Zooplankton		
Zooplankton maximum grazing rate	g	day^{-1}
Zooplankton half saturation constant	k_z	mmol m^{-3}
Zooplankton gross growth efficiency	β	
Zooplankton maximum mortality rate	ε	day^{-1}
Zooplankton mortality half saturation constant	$k_{m\varepsilon}$	mmol m^{-3}
Other		
Remineralisation efficiency	τ	
Across thermocline mixing coefficient	m	m day^{-1}
Light attenuation coefficient due to self-shading	k_c	m^2 $(mmol\ N)^{-1}$
Water attenuation coefficient	k_w	m^{-1}

important in terms of the model's purpose (Fasham, 1993) and the ability to adequately constrain parameters and assess model performance with the observational data available.

Very little observational data were available to constrain other physical or biological processes for the period and location of interest. Adding components such as horizontal advection (which requires horizontal gradients in all fields) or other phytoplankton types to the model that cannot be constrained would increase uncertainty in model results (Anderson, 2005). Although simple, the model presented is well constrained and able to reproduce the available observations. Furthermore, increasing model complexity would not necessarily lead to improved model skill. Significant improvement would need to be determined statistically through methods such as the Akaike's Information Criterion (AIC) which account for extra degrees of freedom.

4. Observational data

Mixed layer depths (MLDs) within the study region were estimated from Argo profiling float data (www.coriolis.eu.org) for the period 2001–2007. Estimates were calculated based on a 0.2 °C temperature difference relative to the 10 m depth (de Boyer Montégut et al., 2004) for individual profiles and then averaged into a monthly climatology. Similarly, PAR data were obtained from the 9 km resolution SeaWiFS product (http://oceandata.sci.gsfc.nasa.gov). Pixel data from the study region between 2001 and 2007 were averaged to form a monthly climatology. To determine below mixed layer nutrient concentrations, nitrate and silicate monthly climatology data at 1° resolution were obtained from the World Ocean Atlas 2009 (WOA09; Garcia et al., 2010). Average nitrate and silicate values within the study region were calculated over depth ranges corresponding to the estimated MLD ± 1 standard deviation. Finally, the climatological estimates for MLD, PAR and below mixed layer nutrient concentrations were spline interpolated to obtain smoothly varying daily estimates for model forcing.

Observations were required for comparison to model output in order to calibrate model parameters and to assess model performance. In particular the ability of the model to simulate the dynamics of the dinoflagellate population was a priority. Long time series data providing information on the temporal variability of phytoplankton are sparse, especially regarding dinoflagellates in non-coastal regions. However, the Continuous Plankton Recorder (CPR) survey provides data for dinoflagellates and diatoms throughout the North Atlantic which can be used to investigate relative temporal changes in abundance on seasonal or longer time scales (Richardson et al., 2006).

CPR data within the study region were obtained from the Sir Alister Hardy Foundation for Ocean Science (SAHFOS) and used to compare observed relative seasonal variations in dinoflagellate and diatom groups to model output. Total dinoflagellate and diatom abundances per sample were $\log_{10}(N+1)$ transformed and averaged for each month of each year between 2001 and 2007 (following Head and Pepin, 2010). These monthly data were then used to calculate weighted climatological averages which ensured that years with a high sampling frequency had a larger influence on the mean than those with a low sampling frequency. Climatological averages were then normalised to a zero mean and unit standard deviation z-score (z_j) following the method set out in Lewis et al. (2006),

$$z_j = \frac{\overline{x}_j - \mu}{\sigma_\mu} \quad (1)$$

where $\overline{x}_j$ is the average value for month j, μ is the average of all months over the year and σ_μ is the standard deviation associated with μ (Cheadle et al., 2003). Normalising the data in this way allows the relative seasonal changes in cell abundance captured by the CPR survey to be compared to the relative seasonal change in biomass simulated by the model.

CPR data only provide information on relative changes in abundance. In order to assess how well the model simulates the absolute phytoplankton abundance, chlorophyll data were compared to the total modelled phytoplankton biomass (i.e. diatoms + dinoflagellates). Chlorophyll data were obtained from the standard SeaWiFS product at 9 km resolution, then $\log_{10}$ transformed to ensure an approximate normal distribution, and averaged over the study area to form a monthly climatology for the period 2001–2007.

Model simulated nutrient concentrations were compared to nitrate and silicate monthly climatology data from the World Ocean Atlas 2009 (WOA09). Data were extracted at 1° resolution from within the study region at the depth (10 m) most closely corresponding to the approximate depth at which the CPR instrument is towed (~7 m). As with the chlorophyll data, nutrient data were $\log_{10}$ transformed to ensure an approximate normal distribution and averaged over the study area.

5. Model parameterisation

5.1. Model goodness of fit

The model was assessed on its combined ability to recreate the relative seasonal variation of dinoflagellates and diatoms and the absolute seasonal changes in chlorophyll, nitrate and silicate concentrations. A cost function was used to assess model performance. It provides a non-dimensional value which quantifies the misfit between model output and observations and is therefore indicative of the "goodness of fit" (Allen et al., 2007). The closer the cost function is to zero the better the model is said to perform.

Model outputs for chlorophyll, nitrate and silicate were $\log_{10}$ transformed and monthly averaged for comparison to observations. In addition, model dinoflagellate and diatom state variables were normalised to a zero mean (Eq. (1)) to allow comparison to corresponding normalised CPR abundance data.

The cost function is the sum of the misfits between model output and observations over the 5 different data types. The individual misfit of each data type j is calculated as

$$CF_j = \frac{1}{N}\sum_{n=1}^{12}\frac{\left(y_{jn}-o_{jn}\right)^2}{{\sigma_{jn}}^2} \quad (2)$$

where j represents each of the 5 different data types (nitrate, silicate, chlorophyll, diatom, dinoflagellate), y_{jn} is the averaged model output in month n of data type j, o_{jn} is the averaged observation in month n of data type j, σ_{jn} is the estimated uncertainty associated with o_{jn} and N is the total number of observations within each data type over the year (Allen et al., 2007). The cost function is therefore defined as

$$CF = \sum_{j=1}^{5} CF_j. \quad 3$$

5.2. Optimisation method

Parameterisation of biological models is notoriously problematic. Many parameter values are poorly constrained and often difficult or impossible to determine (Franks, 2009). Parameter optimisation techniques allow parameter values, including those which it might never be possible to measure, to be estimated. There are several optimisation techniques available to modellers (Friedrichs, 2001; Kidston et al., 2011; Schartau and Oschlies, 2003) which allow a set of parameter values (a parameter vector) to be found which minimises the misfit (as represented by the cost function) between model output and a set of calibration data. In this way it is possible to use abundance and environmental data to infer process rates. Here, model parameter values were estimated through the use of a micro-genetic algorithm (μGA) following a similar procedure to Schartau and Oschlies (2003). The μGA is an automated stochastic optimisation technique that operates on a Darwinian principal of "survival of the fittest" and is crudely based on the mechanics of genetics (Carroll, 1996; Goldberg, 1989).

The cost function defined in Eq. (3) was used to assign a cost to parameter vectors within the optimisation process. To ensure parameter estimates gained from the μGA were not unrealistic, upper and lower limits were set for each parameter. These limits defined the range in which the optimiser could search. All parameters in the model were optimised with the exception of the water attenuation coefficient of downwelling irradiance (kw) which was set a priori because it is a well-defined optical property of seawater. Possible ranges for the remaining 18 parameters were determined from the literature. Where no literature values could be found a deliberately broad range was set to ensure that potential values were not excluded. Fixed values and upper and lower bounds to be considered by the μGA for each parameter are shown in Table 2.

5.3. Calibration data

It is good practice to parameterise a model with a different dataset to the one used for model assessment otherwise the predictive skill of the model cannot be fully evaluated in an unbiased manner. However, this procedure is often limited by the availability of adequate data (Janssen and Heuberger, 1995). Observational datasets were considered too small to be split for cross validation purposes. As such, model parameterisation was instead carried out using several sets of synthetic data which were comparable to those that would be obtained through data splitting.

Synthetic data were generated based on the statistical properties of the observational data. First, it was necessary to ensure that observations of chlorophyll, nutrients and phytoplankton in each month were normally distributed (Gaussian distribution). However, environmental observations, particularly those associated with biological processes such as those used here, commonly have a skewed distribution where mean values are low, variances are large and values cannot be negative (Limpert et al., 2001). Such skewed data frequently demonstrate a log-normal distribution where $\log(x)$ is normally distributed. Therefore, observational data were $\log_{10}$ transformed and statistical tests were performed to ensure data now conformed to a Gaussian distribution. Kolmogorov–Smirnov tests were applied to transformed chlorophyll and nitrate monthly data, whilst Shapiro–Wilk tests were used for phytoplankton data as this test is more appropriate for small

Table 2
Parameter ranges defined from the literature for use within the parameter optimisation process.

Symbol	Unit	Parameter Range		Reference
		Min	Max	
Phytoplankton				
μ_1	day^{-1}	0.4	5.9	Reviewed in Sarthou et al. (2005), Smayda (1997)
μ_2	day^{-1}	0.09	2.7	Chang and Carpenter (1994), Juhl (2005), Jeong and Latz (1994), Tang (1996), Hansen et al. (2000), Hansen and Nielsen (1997), Baek et al. (2007), Baek et al. (2008), Smayda (1997)
k_{N1}	mmol m^{-3}	0.1	5.1	Sarthou et al. (2005)
k_{N2}	mmol m^{-3}	0.01	2	Ignatiades et al. (2007), Qasim et al. (1973), Baek et al. (2008), Kudela et al. (2008), Kudela et al. (2010), Seeyave et al. (2009), Kudela and Cochlan (2000)
k_{Si}	mmol m^{-3}	0.2	4	Sarthou et al. (2005)
α_1	$(W\ m^{-2})^{-1}\ day^{-1}$	0.001	0.1	Sarthou et al. (2005), Popova and Srokosz (2009), Marañón and Holligan (1999), Denman and Pena (1999), Fasham (1993).
α_2	$(W\ m^{-2})^{-1}\ day^{-1}$	0.001	0.1	Popova and Srokosz (2009), Marañón and Holligan (1999), Denman and Pena (1999), Fasham (1993).
V_{diatom}	m day^{-1}	0.1	2.5	Sarthou et al. (2005)
m_p	day^{-1}	0.01	0.5	Fasham (1993), Losa et al. (2004), Merico et al. (2004), Sarthou et al. (2005)
k_{mp}	mmol m^{-3}	0	1	
Zooplankton				
g	day^{-1}	0.4	3	Losa et al. (2004), Fasham (1993), Petzoldt et al. (2009), Odate and Imai (2003), Obayashi and Tanoue (2002)
k_z	mmol m^{-3}	0.01	3	Losa et al. (2004), Sarmiento et al. (1993), Fasham (1993)
β		0.1	1	Evans and Parslow (1985), Fasham (1993)
ε	day^{-1}	0.01	0.5	Losa et al. (2004), Sarmiento et al. (1993), Fasham (1993), Edvardsen et al. (2002)
k_{mz}	mmol m^{-3}	0	0.55	
Other				
τ		0.001	1	
m	m day^{-1}	0	0.01	Upper limit taken from Fasham (1993)
k_c	m^2 (mmol N)$^{-1}$	0.01	0.2	Fasham (1993)

Symbol	Unit	Value	Reference
Fixed parameters			
k_w	m^{-1}	0.04	Fasham (1993), Schartau and Oschlies (2003)

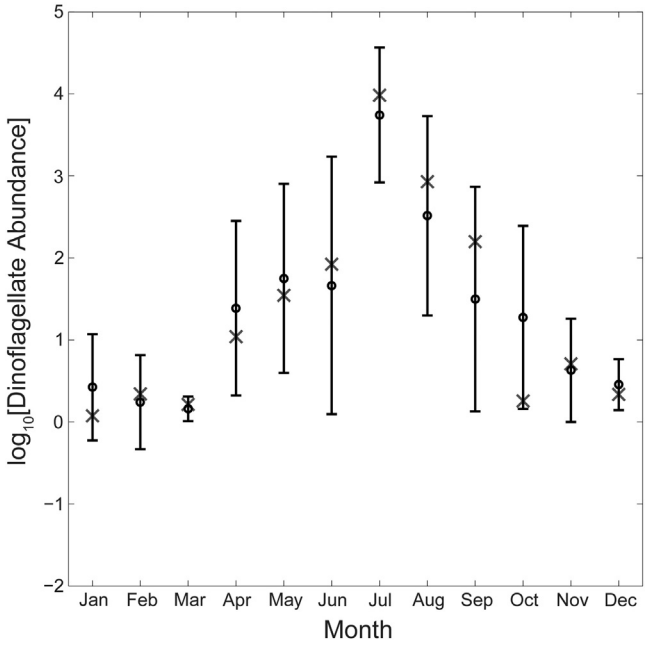

Fig. 4. Example of averaged synthetic dinoflagellate abundance data (x) in comparison to averaged true observational data (o) and associated uncertainty.

sample sizes ($n < 50$). Statistical significance was considered at the 95% ($p < 0.05$) confidence level. Statistical tests and Quantile–Quantile (Q–Q) plots (not shown) indicated that $\log_{10}$ transformed observations were consistent with Gaussian distributions, well described by calculated averages and associated standard deviations.

Synthetic data were generated by randomly selecting a number of data points, equal to the number of real observations, from Gaussian distributions with the same statistical properties of the log transformed observational data. The synthetic data were then averaged and normalised in the same way as their corresponding real observations to produce a synthetic dataset. An example of synthetic dinoflagellate abundance data is shown in Fig. 4 and indicates that synthetic data retains the broad seasonal trend present in the observational data. An advantage of using synthetic data generation is that it allows a large number of calibration datasets to be obtained, without decreasing the size of the dataset used for model assessment.

Table 3
Parameter vectors obtained from model optimisation to the four synthetic data sets. Parameter vector 1 is the optimal set of parameters found through the calibration process.

Parameter	Parameter vector 1 (best)	Parameter vector 2	Parameter vector 3	Parameter vector 4
Phytoplankton				
μ_1	1.45	2.58	3.19	1.53
μ_2	0.46	0.55	0.92	0.59
k_{N1}	0.34	4.70	2.64	0.34
k_{N2}	0.07	0.17	0.51	0.39
k_{Si}	2.37	2.49	1.89	1.59
α_1	0.10	0.10	0.10	0.08
α_2	0.06	0.10	0.087	0.05
V_{diatom}	0.82	1.17	0.10	1.89
m_p	0.25	0.44	0.35	0.27
k_{mp}	0.68	0.75	1.00	0.90
Zooplankton				
g	1.43	2.55	1.10	2.79
k_z	1.72	2.48	1.81	1.72
β	0.89	0.60	0.86	0.57
ε	0.49	0.38	0.31	0.36
$k_{m\varepsilon}$	0.17	0.04	0.23	0.01
Other				
τ	0.51	0.63	0.60	0.41
m	0.01	0.00	0.00	0.0008
k_c	0.03	0.05	0.07	0.09

5.4. Parameterisation

To parameterise the model, four synthetic datasets were generated. The model was optimised to each synthetic dataset in turn, using the μGA, to obtain four optimised parameter vectors (Table 3). The model was then run using each of the optimised parameter vectors and compared to each of the synthetic datasets using the cost function (Eq. (2)). Parameter vector one led to the lowest total cost when summed over all four synthetic datasets and was therefore considered to perform best.

By cross comparing optimised parameter sets tuned to different synthetic data in this way, a set of parameters were identified that best recreated the broad scale variability in the system. Thus, parameterisation of the model was achieved with limited over-fitting to small scale variances caused by uncertainty in the observed data (i.e. measurement noise) whilst ensuring that the broad scale seasonal variation is reproduced. This is an important step when developing models for operational purposes with limited data available.

Table 3 indicates that optimum values of several parameters were highly variable across the four optimised parameter vectors. Despite the variability in many of the parameters, some consistent trends in parameterisation were evident. For example, diatom maximum growth rate (μ_1) was always greater than dinoflagellate maximum growth rate (μ_2), dinoflagellate initial P–I slope (α_2) was never larger than diatom initial P–I slope (α_1) and dinoflagellate nitrate half saturation constant (k_{N2}) was always less than 1 mmol N m^{-3}.

6. Model dynamics

Model output obtained using the optimal parameter set is shown in Fig. 5. As the MLD shoals and PAR increases in early spring (April), diatoms are able to take early advantage of the improving environmental conditions and increase in biomass, due to their lower affinity for light. This population growth of diatoms leads to a draw down in both nitrate and silicate. Dinoflagellates with their higher affinity for light, increase in abundance as the diatoms peak and begin to decline due to increasing silicate limitation. Their lower affinity for nitrate allows dinoflagellates to uptake nitrate more efficiently at lower concentrations.

The dinoflagellate population begins to decline in August as nitrate levels are drawn down and growth rates become nutrient limited. However, as the MLD deepens in September, nutrient levels increase due to mixing. This increase in nutrients causes an autumnal increase in both phytoplankton types. Dinoflagellates gain a greater advantage from the increase in nutrient concentration as their stock biomass in September is much higher than that of diatoms which, because of silicate limitation during late summer, have decreased to a very low level.

It is interesting to note that modelled dinoflagellate biomass stays relatively high throughout the year in comparison to diatoms (Fig. 5). Although diatoms dominate the phytoplankton in April and May, dinoflagellates dominate at all other times of the year and the magnitude of the summer peak in dinoflagellate biomass is larger than that of the spring diatom peak. Losses in biomass of both phytoplankton groups are dominated by zooplankton grazing rather than by natural mortality, indicating that zooplankton are the primary control upon phytoplankton biomass (data not shown).

Seasonal changes in zooplankton track changes in phytoplankton biomass (Fig. 5). Zooplankton grazing contributes significantly to the decline of dinoflagellates during August when the zooplankton grazing rate exceeds the dinoflagellate growth rate. A high gross growth efficiency coefficient (β) means much of the phytoplankton biomass grazed is available for zooplankton growth which leads to increased grazing pressure.

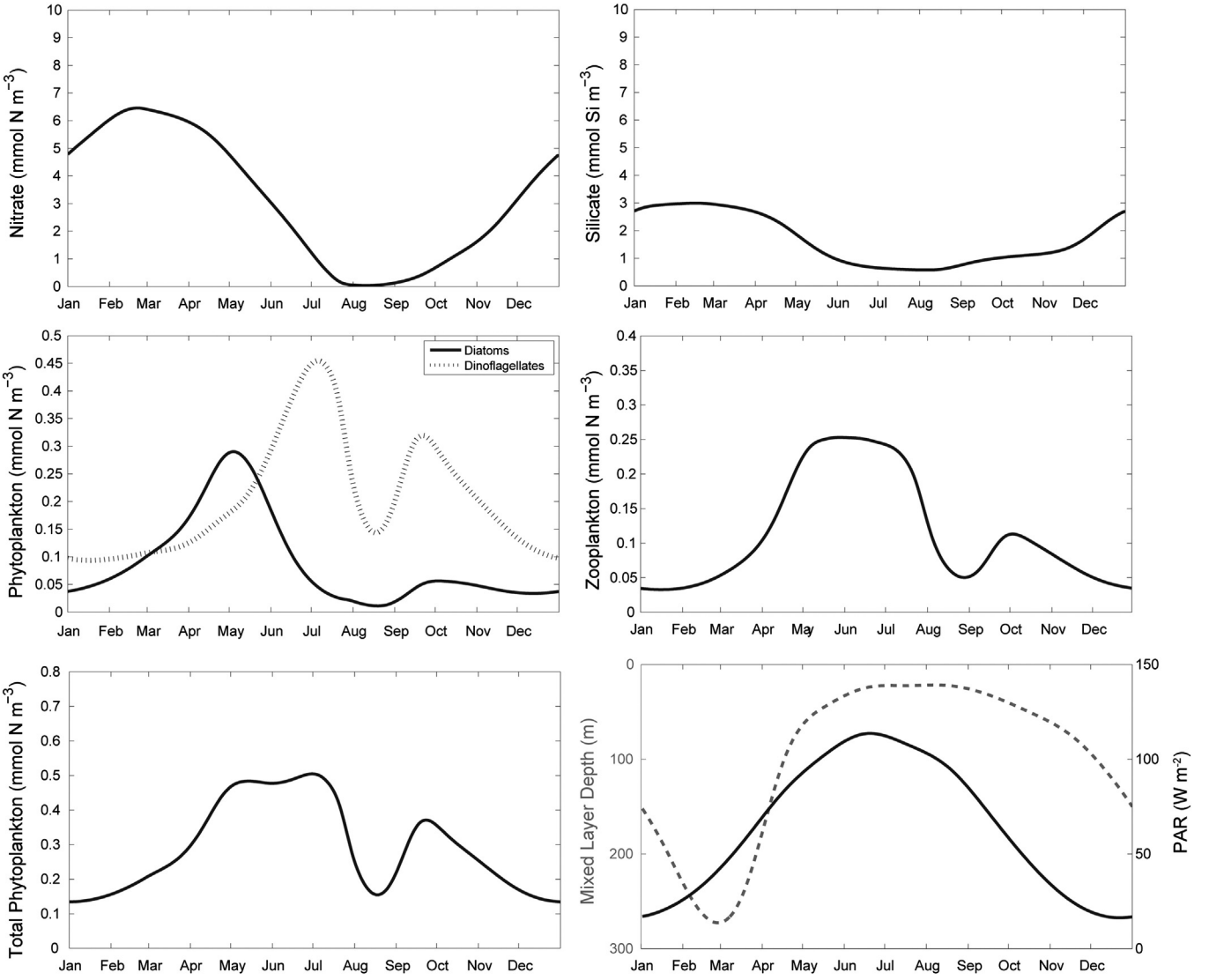

Fig. 5. Model simulations of seasonal changes in nitrate, silicate, diatom and dinoflagellate biomass, zooplankton biomass and total phytoplankton biomass are shown (reading left to right) for a typical year (2001–2007) in the waters surrounding the Porcupine Abyssal Plain observatory. The bottom right plot shows mixed layer depth (dashed line) and photosynthetically active radiation (solid line) used to force seasonal changes.

7. Model assessment

Monthly averaged outputs are compared to the climatologically averaged observations in Fig. 6. The cost function (Eq. (3)), which quantifies the overall misfit between model simulations and observations is equal to 1.87. The contribution of the individual data types to the cost function (CF_j; Eq. (2)) are shown in Table 4. These individual components can be used to assess the model's ability to simulate the different observations. Assessment can be made using performance criteria that are subjectively scaled by the number of standard deviations that model simulations are away from the observations (Allen et al., 2007). Here, model assessment is made using the performance criteria suggested by Radach and Moll (2006) for a cost function as defined in Eq. (2). These criteria are: $CF_j < 1$ is considered very good, 1–2 is good, 2–3 is reasonable and >3 is poor. These criteria are refined from those originally proposed by OSPAR Commission (1998).

Fig. 6 shows that the model is able to accurately replicate the timing of the main peak in seasonal variability for dinoflagellates (June/July) and diatoms (April/May) in the study region. The simulated nutrient and chlorophyll cycles also generally agree well with observations. All model variables for which comparable data were available are classified as very good ($CF_j = <1$), using the criteria suggested by Radach and Moll (2006).

Modelled seasonal variation in dinoflagellates shows two peaks, one in mid-summer and a second in autumn. The summer peak corresponds well to the pattern in the observations, whereas the autumnal peak is not so obvious in the observations, which shows the slow continuous decline of dinoflagellates into winter. The model value for dinoflagellates in August lies just outside of the lower uncertainty boundary of the observations and is responsible for the two peak pattern observed. The model correctly predicts the seasonal pattern in diatoms showing a peak in early spring. However, a comparison to observations indicates that the modelled spring diatom bloom may decline too quickly.

Modelled chlorophyll has a broad primary peak over the spring and summer months spanning both diatom and dinoflagellate blooms. Maximum chlorophyll concentration occurs in June with a secondary peak in autumn (September). This pattern is not exactly equivalent with the observations as the modelled primary peak lags the observations by two months. However, there are only small differences in average observed chlorophyll concentrations between April and June and large associated uncertainties. The secondary autumnal peak in the modelled chlorophyll precedes that in the observations by one month.

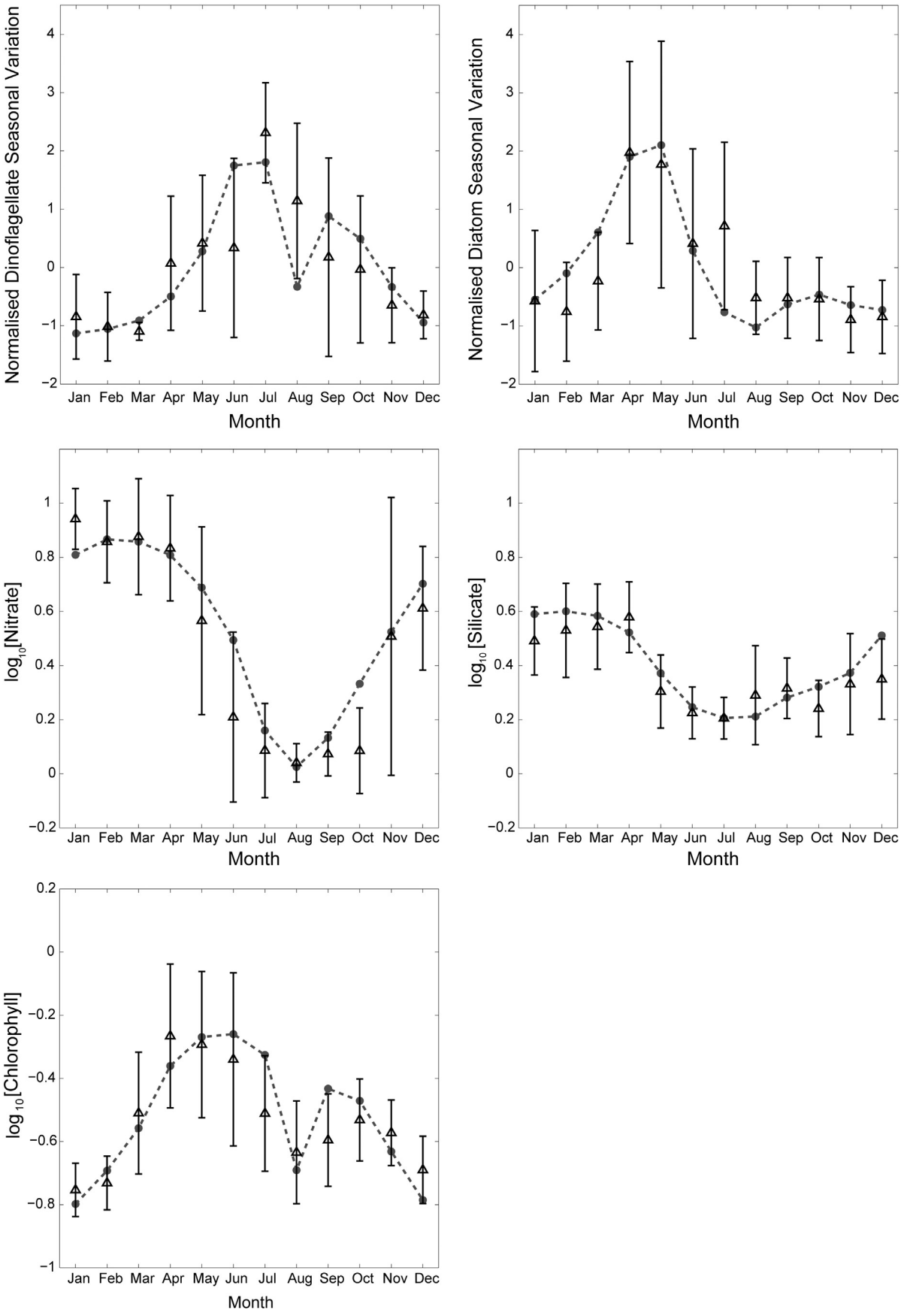

Fig. 6. Comparison of averaged model output (dashed lines and solid circles) against climatologically averaged observations (black triangles).

Table 4
Breakdown of cost indicating misfit between model simulations and observations.

Model forcing	Nitrate	Silicate	Diatoms	Dinoflagellates	Chlorophyll	Total cost
Climatology	0.48	0.29	0.30	0.42	0.38	1.87

Modelled mixed layer nitrate concentrations are higher than average observations through May to December. However, concentrations in all months, with the exception of October, are within the variability of the observations. Simulated silicate concentrations in the summer months of June and July are well matched to their corresponding observations. Modelled silicate is higher than observations through October to March but still falls within the observational variability, with the exception of the December concentration.

8. Modelling inter-annual changes

Given the relatively accurate simulation of the typical seasonal cycle (2001–2007) in dinoflagellate abundance, model analysis was extended to investigate the ability to simulate inter-annual variations over the same period. Monthly values of MLD and PAR were calculated within each year from ARGO float and SeaWiFS data respectively. Due to there being only limited direct measurements of nutrients over the study period, below mixed layer nitrate and silicate concentrations were again estimated from the WOA09 by taking the monthly climatological value at depths corresponding to below the mixed layer. MLD, PAR and nutrient data were once again spline interpolated to daily values (Fig. 7f). Model runs for inter-annual simulations were initialised from the end of a standard 10 year climatological run and used the best performing parameter vector (Table 3). Monthly averaged model output was compared to inter-annual monthly observations using the cost function as in the previous section.

Results show that model simulations are robust and can withstand small changes in forcing (Fig. 7a–e). A breakdown of the cost function indicating the misfit between monthly averaged model simulations and observations from 2001 to 2007 is shown in Table 5. Initially, the ability of the model to simulate inter-annual changes in dinoflagellate and diatom abundance looks poor with cost values >3 (Radach and Moll, 2006). However, on closer investigation the large costs can be attributed to just two months in 2004 and 2007 (circled in Fig. 7a and b). Particularly large costs are associated with the inability of the model to simulate the increase of dinoflagellates and diatoms in September 2004 (and similarly the increase of diatoms in July 2007) because only small uncertainties are related to the averaged monthly data. It is worth noting that only a few samples (2 and 5) make up the average for these months. Thus, it is possible that the uncertainty on these observations is substantially underestimated. Removing the three data points in question and recalculating the cost function indicates that model simulations are still classed as very good (<1) or good (1–2) (Table 5).

9. Example BPOT forecast

Within this section the potential for using output from the model developed in the previous sections to forecast seasonal changes in BPOT is illustrated. To estimate BPOT from model output a relationship between BPOT and dinoflagellate nitrogen biomass must be determined. Given the lack of BPOT observations with simultaneous abundance/biomass data, we determine such a relationship indirectly based on information contained within the CPR data for the PAP study area. The dinoflagellate abundance data from the CPR survey can be broken down to genera and species level. This allows species that are known to be bioluminescent to be identified and an estimate of how BPOT may vary over a typical year to be constructed.

Light budgets were calculated by multiplying cell abundances of bioluminescent species by their approximate flash intensities. *Gonyaulax* spp. and *Ceratium fusus* were taken to have flash intensities of 1×10^8 photons s^{-1} whilst *Protoperidinium* spp. were assumed to flash at an intensity of 1×10^9 photons s^{-1} (as in Swift et al., 1995). Summing the calculated bioluminescence potential of each genera or species gives an estimate of the BPOT in each month. Over the 2001–2007 climatology a strong positive linear relationship ($r^2 = .974$; $p < .001$; $n = 12$) is found between estimated BPOT and total dinoflagellate abundance within the PAP study region. An assumption can then be made that, to first order, cell abundance is directly proportional to biomass such that $Biomass = c[Cell\ Abundance]$, where c is a constant factor representing the average carbon content per cell. Based on experimental data across 20 different dinoflagellate species an average per cell carbon content of 6364 pg C $cell^{-1}$ is assumed (Menden-Deuer and Lessard, 2000). Using a C:N ratio of 6.625 this is equivalent to 961 pg N $cell^{-1} = 6.86 \times 10^{-8}$ mmol N $cell^{-1}$. Using this factor, CPR cell abundance is converted to nitrogen biomass and a linear correlation exists between BPOT and nitrogen biomass, as shown in (Fig. 8a). A linear regression indicates that BPOT can be approximated by the equation $BPOT = -8.246 \times 10^{10} + (1.369 \times 10^{15} * \text{biomass})$ with an $r^2 = 0.974$ ($p < .001$). This relationship can be used to provide a forecast of the seasonal change in BPOT given the modelled dinoflagellate biomass as demonstrated in Fig. 8b.

The example presented here is purely a demonstration based on a model hindcast specific to the Porcupine Abyssal Plain. However, it illustrates the potential for this approach to be applied to forecasting the seasonal changes in BPOT in future given predictions of the physical environment. Furthermore, comparable model and statistical relationships derived from observations could be applied more widely to other regions of the North Atlantic. Indeed, the observations of dinoflagellate abundance are readily available across the North Atlantic from the CPR survey.

10. Discussion

The complex and dynamic interactions between bioluminescent plankton, their environment and other organisms have limited the success of previous attempts to forecast bioluminescence in the North Atlantic using static relationships between BPOT and variables such as temperature and chlorophyll (e.g. Ondercin et al., 1995). Modelling the ecological dynamics of bioluminescent organisms and their reactions to changes in environment offers a more robust way to forecast the spatial and the temporal distribution of bioluminescence (reviewed by Marcinko et al., 2013a). Positive associations between BPOT and total dinoflagellate cell abundance including bioluminescent and non-bioluminescent species, found across several regions (Kim et al., 2006; Lapota et al., 1989; Tokarev et al., 1999), indicate that total dinoflagellate abundance can be used as a proxy for BPOT. Given that species of these organisms are responsible for the majority of bioluminescence stimulated in the surface ocean of the North Atlantic (Swift et al., 1995), the simple model described above, which is able to simulate dinoflagellate abundance, potentially provides a platform for the future seasonal forecasting of bioluminescence.

The model provides a very good fit to monthly climatology observations and is able to recreate both the typical seasonal peak in dinoflagellates and diatoms. However, one concern is that simulations show a two month lag exists between simulated and observed peak chlorophyll concentrations as a consequence of dinoflagellate biomass in summer being greater than that of diatoms in spring. This suggests that the model underestimates peak diatom biomass or overestimates peak dinoflagellate biomass. Unfortunately, observational data are not available to directly compare to simulated biomass estimates of the individual phytoplankton groups. Nonetheless model results are supported by data shown by Taylor et al. (1993) taken around 47°N 20°W during May to August 1989, which indicate that estimates of summer dinoflagellate

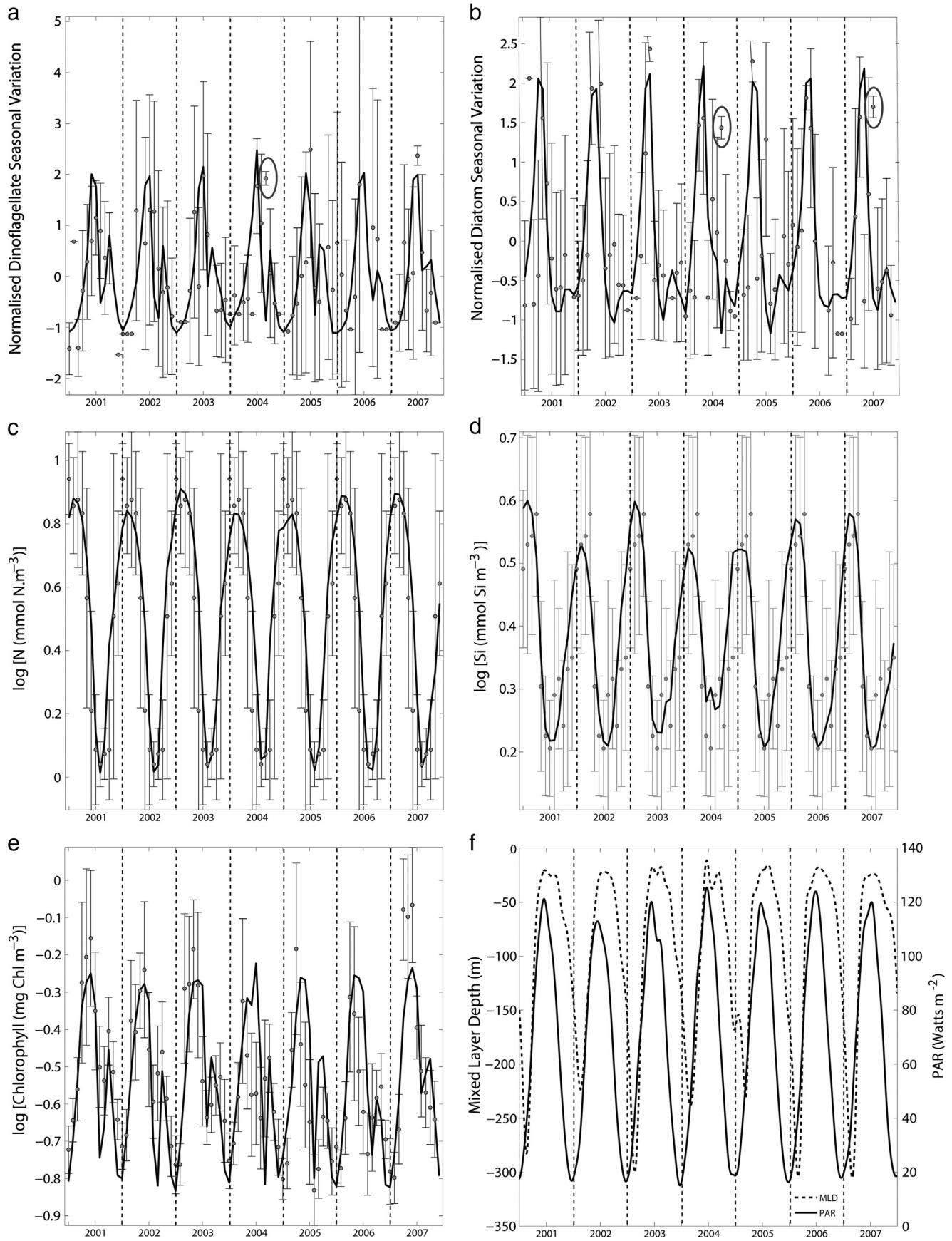

Fig. 7. Comparison between inter-annual model simulations and observational data for (a) normalised seasonal variation in dinoflagellates (b) normalised seasonal variation in diatoms (c) nitrate (d) silicate (e) chlorophyll and (f) inter-annual forcing of MLD and PAR between January 2001 and December 2007.

Table 5
Breakdown of cost indicating the misfit between inter-annual model simulations and observations.

Model forcing	Nitrate	Silicate	Diatoms	Dinoflagellates	Chlorophyll	Total cost
Inter-annual	0.52	0.24	9.48	6.57	1.54	18.35
Inter-annual (Sep 2004 & Jul 2007 removed)	0.52	0.24	0.82	0.46	1.54	3.58

biomass (~50 mg C m^{-3} in mid-July) were slightly higher than those for the diatom bloom in late spring (~45 mg C m^{-3} in mid-May). Laboratory studies have also indicated that larger dinoflagellates are more carbon dense than larger diatoms (Menden-Deuer and Lessard, 2000). It is also possible that the model structure limits its ability to match the exact observational pattern in chlorophyll because it does not consider other phytoplankton groups such as fast growing phytoflagellates or coccolithophores, which may contribute to the chlorophyll signal in early spring and summer, respectively.

Several parameters show significant variability across the calibrated parameter vectors (Table 3), suggesting some under-determination of the system. Uncertainty in the parameter values arises from both variability in the observations and potential deficiencies of the optimisation method and model structure (Schartau and Oschlies, 2003). Some of the variability across parameter vectors could be due to the size of the parameter ranges used in the optimisation procedure, which were deliberately broad to ensure that potential values were not excluded (Table 2). Despite the variability across different parameter vectors, several trends were consistent and agree with known physiological traits of the phytoplankton types. For example, dinoflagellate maximum growth rate was always lower than that of diatoms, in agreement with knowledge that dinoflagellates have lower maximum growth rates than other phytoplankton types of similar size (Banse, 1982; Litchman et al., 2007). Also, the initial P–I slope of diatoms (α_1) was never lower than that of dinoflagellates (α_2) in agreement with knowledge that diatoms are known to generally be better adapted to low-light characteristics (Le Quere et al., 2005; Litchman et al., 2007).

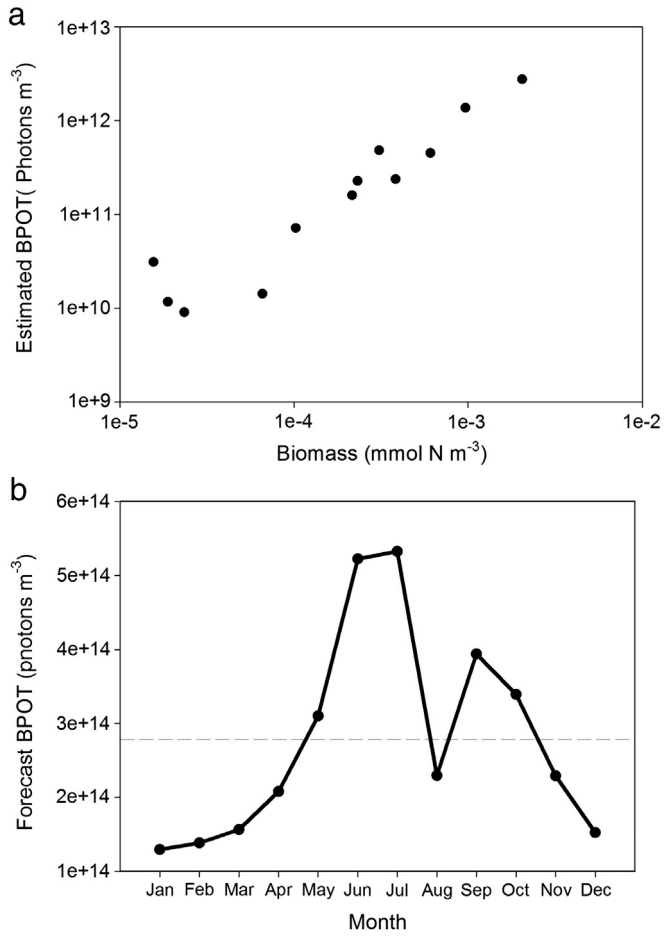

Fig. 8. a) Relationship between CPR derived BPOT estimates and dinoflagellate biomass climatology from the PAP study area between 2001 and 2007 (axes are $\log_{10}$ scaled). b) Example forecast of BPOT based on modelled dinoflagellate biomass (dashed horizontal line indicates seasonal mean).

10.1. Forecasting bioluminescence

Section 9 illustrates how the modelled seasonal changes in dinoflagellate abundance can potentially be used to estimate expected BPOT at a particular time of year. This was achieved through combining simulated dinoflagellate biomass data with a statistically derived relationship between observed dinoflagellate abundance and BPOT. However, it must be noted that the estimation of BPOT made here has a number of limitations. CPR data are known to underestimate cell abundance due to the sampling procedure and this particularly affects unarmoured dinoflagellates. Therefore, results may be biased towards the armoured dinoflagellate population and likely substantially underestimate the concentration of bioluminescent cells. Also, in the process of calculating BPOT it is assumed that all cells within a bioluminescent genera or species will luminesce to their full potential. However, bioluminescent and non-bioluminescent strains of the same species can exist and the physiological state of a cell can influence its bioluminescent intensity (Buskey et al., 1994; Latz and Jeong, 1996). Therefore, the modelled BPOT may be lower than calculated. This may be particularly true towards the end of a bloom when cells become nutritionally stressed but are still in high abundance.

Despite the crudeness of the calculations made in Section 9, it is encouraging to note that the bioluminescent intensities predicted in this example study are consistent with measurements made during the Marine Light Mixed Layer programme, which found BPOT to vary between approximately 1×10^{14} and 4×10^{14} photons m^{-3} between May and September within the North Atlantic Irminger Sea (Swift et al., 1995). However, further observations are required to determine a well defined relationship between dinoflagellate abundance and measured BPOT. At present, model calibration and validation are significantly limited by a lack of spatial and seasonal bioluminescence data. The recent development of commercially available bathyphotometers that can be attached to towed platforms and fixed moorings offers the potential to increase measurement frequency of bioluminescence in the future and efforts should be made to secure sustained observations with the necessary coincident biological data, particularly at key points in the seasonal cycle such as spring and autumn.

Measured BPOT intensities are highly instrument dependent and vary given different flow rates and stimulation mechanisms. Therefore, forecasting exact BPOT intensities stimulated and experienced by an individual observer may be somewhat impractical. However, predicted seasonal changes in dinoflagellate abundance could be used to estimate the probability of encountering bioluminescence at a particular time of year. Model output can be combined with a probability scale, set relative to the magnitude of dinoflagellate abundance above a typical annual mean. An increase in dinoflagellate biomass above the set threshold would be associated with an increased presence of bioluminescent cells and associated with a higher than average likelihood of encountering bioluminescence at this time of year.

Given that previous research has indicated that forecasting bioluminescence on time scales of hours to days may be heavily dependent on

modelling its relationship with localised light conditions (Marcinko et al., 2013b; Sullivan and Swift, 1995; Sweeney, 1981). The simple example highlighted in Section 9 could be further progressed through combining finer temporal resolution model output with a bioluminescence algorithm such as that used by Ondercin et al. (1995), which estimates BPOT within the mixed layer as a function of both simulated dinoflagellate biomass and instantaneous solar irradiance at the sea surface.

10.2. Future model development

Results have demonstrated the ability of the model to simulate the seasonal changes in the dinoflagellate population within an area of the Northeast Atlantic, despite its relative simplicity. However, further development and testing of the model in locations other than the study region will be required before applying it to the wider North Atlantic. At present it is not clear to what extent the structural simplicity of the model may hamper its predictive skill in other locations. The model lacks terms representing a detrital pool or microbial loop (bacteria), which could restrict accurate simulation of recycled nutrient availability (Anderson, 2010). These terms may be particularly important in oligotrophic regions (such as the subtropical North Atlantic) where nutrient availability is heavily dependent upon recycling in the surface layer. The restriction of the model to the mixed layer may also be an issue in such regions, where there may be a significantly deeper phytoplankton community.

The addition of other phytoplankton types, such as small flagellates may improve simulations of chlorophyll and absolute dinoflagellate biomass as in situ observations have shown that they can make up a significant amount of the pre- and post-bloom chlorophyll within the North Atlantic (Sieracki et al., 1993; Verity et al., 1993). Correspondingly, the inclusion of protozooplankton may be required for more accurate representation of the nutrient transfer between small phytoplankton and metazooplankton. Furthermore, the inclusion of protozooplankton may improve simulations of recycled nutrient availability as they are thought to have an important role in the cycling of organic matter in oceanic waters (Verity et al., 1993).

There is some evidence to suggest that greater phytoplankton complexity within ecosystem models can generate enhanced portability (Friedrichs et al., 2007) but this comes at a price. Increasing model complexity requires additional observations to constrain parameters and assess simulations. Additions to the model structure will need to balance the cost in uncertainty and greater need for data against the benefits to potential predictive skill. The lack of abundance data for individual phytoplankton groups is known to hinder the calibration and validation of multiple phytoplankton functional type (PFT) models (Hofmann, 2010). However, methods to identify PFTs from satellite derived datasets are continually advancing and may, in future, provide data for robust model testing of the horizontal distributions of specific phytoplankton types such as dinoflagellates (Aiken et al., 2007; Alvain et al., 2008; Raitsos et al., 2008).

Forecasting dinoflagellates on finer horizontal scales, with the front and eddy populated mesoscale of particular interest or below the mixed layer, will require the model structure to be coupled with a more detailed physical model that accurately represents changes in the physical environment at the required spatial scale. This may be achieved by implementing the model into a 3-D ocean general circulation modelling (GCM) framework such as NEMO (Nucleus for European Models of the Ocean; Madec, 2008).

The model presented in this study, although simple in terms of structure, provides a first step in developing simulations of the broad temporal and spatial changes in dinoflagellate abundance across the North Atlantic. Given the example set out in Section 9 of how such simulations could provide a feasible approach to estimating seasonal changes in BPOT, this model can provide a solid platform to work from for the future operational forecasting of BPOT.

11. Conclusion

The capability to reproduce much of the seasonal variation in bioluminescence within the North Atlantic, even if at course resolutions, would be a significant step forward. Forecasting bioluminescence potential through modelling the distribution of a specific bioluminescent phylum has not previously been attempted. The ability to forecast where and when bioluminescence is most likely to occur, even if the intensity itself cannot be estimated, would provide valuable information, currently not available, that may permit enhanced decision making and enable targeted field campaigns.

This study aimed to develop an ecological based model that could be used as a first step in operational forecasting of BPOT. The model successfully simulates broad temporal changes in dinoflagellates (the planktonic group responsible for the majority of bioluminescence observed in surface ocean) for the waters surrounding the Porcupine Abyssal Plain in the Northeast Atlantic. The study has illustrated that forecasting BPOT may be possible through combining the output of a relatively simple ecological model with frequently observed statistical relationships between BPOT and dinoflagellate cell abundance. However, further observations of BPOT with coincident dinoflagellate cell abundance data are essential for accurate model validation and prediction. The ability of such an approach to be applied to a wider geographical region has been discussed and, although further work is needed, the model developed here offers a promising platform for the future operational forecasting of bioluminescence in the North Atlantic.

Acknowledgments

We acknowledge the Ministry of Defence for their financial support of this project under the Joint Grant Scheme programme (proposal ref: 1166) and the Natural Environmental Research Council's commitment to the U.K.'s marine research capability through the Oceans 2025 programme and NC funding. We thank the Sir Alister Hardy Foundation for Ocean Science (SAHFOS), David Johns and Darren Stevens and for providing access to, and advice on, data from the Continuous Plankton Recorder (CPR) Survey and funding through the SAHFOS associate researcher bursary scheme. We also thank Martin Dohrn and his colleagues at Ammonite Films for providing the image used as Fig. 1.

Appendix A

Mixed layer depth

Changes in the depth of the mixed layer (M), imposed from observations, are a function of time (t) in days and are calculated as

$$h(t) = \frac{dM}{dt}. \quad \text{A.1}$$

A positive change in M caused by a deepening in MLD, defined by $h^{+}(t)$ (Eq. (A.2)), produces entrainment and mixing of nutrients from the deep abiotic layer into the upper mixed layer.

$$h^{+}(t) = max(h(t), 0). \quad \text{A.2}$$

Phytoplankton

The differential equations for phytoplankton state variables have a common form following

$$\frac{dP}{dt} = Grow - Mort - Graz - Mix - Sink \quad \text{A.3}$$

where *Grow* is the gain in phytoplankton due to population growth, *Mort* parameterises all losses through non-grazing activity including

natural mortality, *Graz* is the loss due to zooplankton grazing, *Mix* is the loss due to changes in *M* and *Sink* is the loss due to cells sinking out of the mixed layer.

Phytoplankton growth is a function of both nutrient and light limitations. The nutrient limited growth of dinoflagellates (P_2) is controlled by the availability of nitrate (Eq. (A.4)), whereas for diatoms (P_1) it is influenced by both nitrate and silicate (Eq. (A.5)).

$$Grow_{P_2} = J_2 \frac{N}{N + k_{N2}} P_2 \tag{A.4}$$

$$Grow_{P_1} = J_1 \left[min\left(\frac{N}{N + k_{N1}}, \frac{Si}{Si + k_{Si}} \right) \right] P_1 \tag{A.5}$$

where k_{N1} and k_{Si} are the half saturation constants for nitrate and silicate for P_1, k_{N2} is the half saturation constant for nitrate for P_2 and J_1 and J_2 are the light-limited growth rates for P_1 and P_2, respectively, calculated following Evans and Parslow (1985).

Mort, *Graz* and *Mix* terms for a specified phytoplankton type *j* are given by

$$Mort_{Pj} = \frac{m_p {P_j}^2}{k_m + P_j} \tag{A.6}$$

where m_p is the maximum natural phytoplankton mortality rate and k_m is the half saturation constant for phytoplankton mortality.

$$Graz_{Pj} = g\left(\frac{P_j}{k_z + P_1 + P_2} \right) Z \tag{A.7}$$

where *g* is the zooplankton maximum ingestion rate and k_z is the half saturation constant for grazing.

$$Mix_{Pj} = \frac{(m + h^+(t)) P_j}{M} \tag{A.8}$$

where *m* represents the mixing due to turbulence between the upper mixed layer and the deeper abiotic layer.

Diatoms actively sink from surface waters. As such, within the model P_1 are assumed to sink from the upper mixed layer as represented by the *Sink* term in Eq. (A.3) controlled by a constant sinking rate V_{diatom}. Dinoflagellates are not considered to actively sink and the model assumes that P_2 remains within the upper mixed layer when there is a shoaling or no change in *M*. Hence the *Sink* term for P_2 is set to zero.

Zooplankton

The zooplankton (*Z*) differential equation has the form

$$\frac{dZ}{dt} = Grow_Z - Mort_Z - Mix_Z \tag{A.9}$$

where $Grow_Z$ is the gain in zooplankton due to population growth through grazing upon phytoplankton, $Mort_Z$ is the loss due to zooplankton mortality, and Mix_Z represents changes in zooplankton concentration due to the varying depth (*M*) of the mixed layer.

The $Grow_Z$ term assumes that zooplankton effectively has equal grazing preference for P_1 and P_2 phytoplankton types and is defined by

$$Grow_Z = g\beta\left(\frac{P_1 + P_2}{k_z + P_1 + P_2} \right) Z \tag{A.10}$$

where *g* is the zooplankton maximum specific grazing rate, β is the assimilation efficiency and k_z is the half saturation constant for grazing.

Grazed material that is not assimilated by zooplankton for growth is assumed lost via messy feeding (MF_Z) and available for remineralisation back into the nutrient pool. MF_Z is given as

$$MF_Z = (1-\beta) g\left(\frac{P_1 + P_2}{k_z + P_1 + P_2} \right) Z. \tag{A.11}$$

The mortality term for zooplankton is the effective closure term of the model and represents the losses due to both natural mortality and higher predators which are not explicitly modelled. The $Mort_Z$ term follows the hyperbolic form given in Fasham (1993)

$$Mort_Z = \frac{\varepsilon Z^2}{k_{mz} + Z} \tag{A.12}$$

where ε is the zooplankton maximum mortality rate and k_{mz} is the half saturation constant for the zooplankton mortality rate.

The Mix_Z term concentrates or dilutes zooplankton with the shoaling or deepening of the MLD, respectively. Mix_Z is given as

$$Mix_Z = \frac{Zh(t)}{M}. \tag{A.13}$$

Nitrate

The differential equation for nitrate takes the form

$$\frac{dN}{dt} = \tau\left(Mort_Z + Mort_{P_1} + Mort_{P_2} + MF_z \right) - Grow_{P_1} - Grow_{P_2} + Mix_N. \tag{A.14}$$

As no detritus pool is explicitly modelled, a constant fraction τ of the material lost from phytoplankton and zooplankton through mortality and messy feeding is remineralised directly into the nutrient pool. The remineralisation efficiency τ sets the export rate from the biologically active upper layer into the abiotic deep layer. All material not remineralised (equal to $(1-\tau)\left[Mort_Z + Mort_{P_1} + Mort_{P_2} + MF_z\right]$) effectively disappears from the model domain and should be considered exported, either to higher predators or below the mixed layer.

The Mix_N term specifies the increase in nitrate due to a deepening of the MLD and is given as

$$Mix_N = \frac{(m + h^+(t))}{M} (N_0 - N) \tag{A.15}$$

where N_0 is the nitrate concentration bow the mixed layer.

Silicate

The differential equation for silicate takes the form

$$\frac{dSi}{dt} = \left[\tau\left(Mort_{P_1} + Graz_{P_1} \right) - Grow_{P_1} \right] / R_{N:Si} + Mix_{Si} \tag{A.16}$$

where Mix_{Si} represents the gain in silicate due to mixing and $R_{N:Si}$ is the N:Si ratio. Mix_{Si} follows the same form as the mixing term for nitrate given in Eq. (A.15) replacing *N* and N_0 with *Si* and S_0 respectively.

Within the model zooplankton are assumed not to uptake silicate for growth and therefore all grazed silicate material ($Grow_Z + MF_Z$) is available for remineralisation back into the system.

References

Aiken, J., Fishwick, J.R., Lavender, S., Barlow, R., Moore, G.F., Sessions, H., Bernard, S., Ras, J., Hardman-Mountford, N.J., 2007. Validation of MERIS reflectance and chlorophyll during the BENCAL cruise october 2002: preliminary validation of new demonstration products for phytoplankton functional types and photosynthetic parameters. Int. J. Remote Sens. 28 (3), 497–516.

Allen, J.I., Holt, J.T., Blackford, J., Proctor, R., 2007. Error quantification of a high-resolution coupled hydrodynamic-ecosystem coastal-ocean model: part 2. Chlorophyll-a, nutrients and SPM. J. Mar. Syst. 68 (3–4), 381–404.

Alvain, S., Moulin, C., Dandonneau, Y., Loisel, H., 2008. Seasonal distribution and succession of dominant phytoplankton groups in the global ocean: a satellite view. Glob. Biogeochem. Cycles 22, GB3001.

Anderson, J.T., 1998. The effects of seasonal variability on the germination and vertical transport of a cyst forming dinoflagellate, *Gyrodinium* sp., in Chesapeake Bay. Ecol. Model. 112, 85–109.

Anderson, T.R., 2005. Plankton functional type modelling: running before we can walk? J. Plankton Res. 27 (11), 1073–1081.

Anderson, T.R., 2010. Progress in marine ecosystem modelling and the "unreasonable effectiveness of mathematics". J. Mar. Syst. 81, 4–11.

Baek, S.H., Shimode, S., Kikuchi, T., 2007. Reproductive ecology of the dominant dinoflagellate, *Ceratium fusus* in coastal area of Sagami Bay. J. Oceanogr. 30, 35–45.

Baek, S.H., Shimode, S., Han, M.-S., Kikuchi, T., 2008. Growth of dinoflagellates, *Ceratium furca* and *Ceratium fusus* in Sagami Bay, Japan: the role of nutrients. Harmful Algae 7, 729–739.

Banse, K., 1982. Cell volumes, maximal growth rates of unicellular algae and ciliates, and the role of ciliates in the marine pelagial. Limnol. Oceanogr. 27, 1059–1071.

Barlow, R.G., Mantoura, R.F.C., Gough, M.A., Fileman, T.W., 1993. Pigment signatures of the phytoplankton composition in the Northeastern Atlantic during the 1990 spring bloom. Deep-Sea Res. II 40, 459–477.

Batchelder, H.P., Swift, E., 1989. Estimated near-surface mesoplanktonic bioluminescence in the western North Atlantic during July 1986. Limnol. Oceanogr. 34, 113–128.

Behrenfeld, M.J., Boss, E., Siegel, D.A., Shea, D.M., 2005. Carbon-based ocean productivity and phytoplankton physiology from space. Glob. Biogeochem. Cycles 19 (1), GB1006.

Brzezinski, M.A., 1985. The Si:C:N ratio of marine diatoms: interspecific variability and the effect of some environmental variables. J. Phycol. 21 (3), 347–357.

Buskey, E.J., Coulter, C.J., Brown, S.L., 1994. Feeding, growth and bioluminescence of the heterotrophic dinoflagellate *Protoperidinium huberi*. Mar. Biol. 121, 373–380.

Carroll, D.L., 1996. Chemical laser modelling with genetic algorithms. AIAA J. 34 (2), 338–346.

Chang, J., Carpenter, E.J., 1994. Active growth of the oceanic dinoflagellate *Ceratium teres* in the Caribbean and Sargasso Seas estimated by cell cycle analysis. J. Phycol. 30, 375–381.

Cheadle, C., Vawter, M.P., Freed, W.J., Becker, K.G., 2003. Analysis of microarray data using z-score transformation. J. Mol. Diagn. 5, 73–81.

Churnside, J., Jech, M., Tenningen, E. (Eds.), 2012. Fishery Applications of Optical Technologies. ICES Cooperative Research Report No. 312 (91 pp.).

Cugier, P., Ménesguen, A., Guillaud, J.F., 2005. Three-dimensional (3D) ecological modelling of the Bay of Seine (English Channel, France). J. Sea Res. 54, 104–124.

de Boyer Montégut, C., Madec, G., Fischer, A.S., Lazar, A., Iudicone, D., 2004. Mixed layer depth over the global ocean: an examination of profile data and a profile-based climatology. J. Geophys. Res. 109 (C12), C12003.

Denman, K.L., Pena, M.A., 1999. A coupled 1-D biological/physical model of the northeast subarctic north Pacific Ocean with iron limitation. Deep-Sea Res. II 46 (11–12), 2877–2908.

Dodge, J.D., 1993. Armoured dinoflagellates in the NE Atlantic during the BOFS cruises, 1988–90. J. Plankton Res. 15, 465–483.

Ducklow, H.W., Harris, R.P., 1993. Introduction to the JGOFS North Atlantic bloom experiment. Deep-Sea Res. II 40, 1–8.

Edvardsen, A., Zhou, M., Tande, K.S., Zhu, Y., 2002. Zooplankton population dynamics: measuring in situ growth and mortality rates using an Optical Plankton Counter. Mar. Ecol. Prog. Ser. 227, 205–219.

Evans, G.T., Parslow, J.S., 1985. A model of annual plankton cycles. Biol. Oceanogr. 3 (3), 327–347.

Fasham, M.J.R., 1993. Modelling the marine biota. NATO ASI Ser. I (15), 457–504.

Follows, M.J., Dutkiewicz, S., Grant, S., Chisholm, S.W., 2007. Emergent biogeography of microbial communities in a model ocean. Science 315, 1843.

Franks, P.J.S., 1997. Models of harmful algal blooms. Limnol. Oceanogr. 42, 1273–1282.

Franks, P.J.S., 2009. Planktonic ecosystem models: perplexing parameterizations and a failure to fail. J. Plankton Res. 31 (11), 1299–1306.

Friedrichs, M.A., 2001. A data assimilative marine ecosystem model of the central equatorial Pacific: numerical twin experiments. J. Mar. Res. 59, 859–894.

Friedrichs, M.A., Dusenberry, J.A., Anderson, L.A., Armstrong, R.A., Chai, F., Christian, J.R., Doney, S.C., Dunne, J., Fujii, M., Hood, R., McGillicuddy, D.J., Moore, J.K., Schartau, M., Spitz, Y.H., Wiggert, J.D., 2007. Assessment of skill and portability in regional marine biogeochemical models: role of multiple planktonic groups. J. Geophys. Res. 112 (C8), C08001.

Garcia, H.E., Locarnini, R.A., Boyer, T.P., Antonov, J.I., Zweng, M.M., Baranova, O.K., Johnson, D.R., 2010. World Ocean Atlas 2009. In: Levitus, S. (Ed.), Volume 4: Nutrients (Phosphate, Nitrate, and Silicate). NOAA Atlas NESDIS, 71. U.S. Government Printing Office, Washington, D.C. (398 pp.).

Goldberg, D., 1989. Genetic Algorithms in Search, Optimization, and Machine Learning. Addison-Wesley Professional.

Haddock, S.H.D., Moline, M.A., Case, J.F., 2010. Bioluminescence in the sea. Annu. Rev. Mar. Sci. 2, 443–493.

Hansen, P.J., Nielsen, T.G., 1997. Mixotorphic feeding of *Fragilidium subglobosum* (Dinophyceae) on three species of *Ceratium*: effects of prey concentration, prey species and light intensity. Mar. Ecol. Prog. Ser. 147, 187–196.

Hansen, P.J., Skovgaard, A., Ronnie, N.G., Stoecker, D.K., 2000. Physiology of the mixotrophic dinoflagellate *Fragilidium subglobosum*. II. Effects of time scale and prey concentration on photosynthetic performance. Mar. Ecol. Prog. Ser. 201, 137–146.

Head, E., Pepin, P., 2010. Monitoring changes in phytoplankton abundance and composition in the Northwest Atlantic: a comparison of results obtained by continuous plankton recorder sampling and colour satellite imagery. J. Plankton Res. 32 (12), 1649–1660.

Herring, P.J., Widder, E.A., 2001. Bioluminescence in the plankton and nekton. In: Steele, J. H., Thorpe, S.A., Turekian, K.K. (Eds.), Encyclopedia Of Ocean Science, 1. Academic Press, San Diego, pp. 308–317.

Hofmann, E.E., 2010. Plankton functional group models—an assessment. Prog. Oceanogr. 84, 16–19.

Hood, R.R., Laws, E.A., Armstrong, R.A., Bates, N.R., Brown, C.W., Carlson, C.A., Chai, F., Doney, S.C., Falkowski, P.G., Feely, R.A., Friedrichs, M.A.M., Landry, M.R., Keith Moore, J., Nelson, D.M., Richardson, T.L., Salihoglu, B., Schartau, M., Toole, D.A., Wiggert, J.D., 2006. Pelagic functional group modeling: progress, challenges and prospects. Deep-Sea Res. II 53, 459–512.

Ignatiades, L., Gotsis-Skretas, O., Metaxatos, A., 2007. Field and culture studies on the ecophysiology of the toxic dinoflagellate *Alexandrium minutum* (Halim) present in Greek coastal waters. Harmful Algae 6 (2), 153–165.

Janssen, P.H.M., Heuberger, P.S.C., 1995. Calibration of process-oriented models. Ecol. Model. 83, 55–66.

Jeong, H.J., Latz, M.I., 1994. Growth and grazing rates of the heterotrophic dinoflagellate, *Protoperidinium*, on red tide dinoflagellates. Mar. Ecol. Prog. Ser. 106, 173–185.

Juhl, A.R., 2005. Growth rates and elemental composition of *Alexandrium monilatum*, a red-tide dinoflagellate. Harmful Algae 4 (2), 287–295.

Kidston, M., Matear, R., Baird, M.E., 2011. Parameter optimisation of a marine ecosystem model at two contrasting stations in the Sub-Antarctic Zone. Deep-Sea Res. II 58, 2301–2315.

Kim, G., Lee, Y.-W., Joung, D.-J., Kim, K.-R., Kim, K., 2006. Real-time monitoring of nutrient concentrations and red-tide outbreaks in the Southern Sea of Korea. Geophys. Res. Lett. 33, L13607.

Kudela, R.M., Cochlan, W.P., 2000. Nitrogen and carbon uptake kinetics and the influence of irradiance for a red tide bloom off southern California. Aquat. Microb. Ecol. 21, 31–47.

Kudela, R.M., Lane, J.Q., Cochlan, W.P., 2008. The potential role of anthropogenically derived nitrogen in the growth of harmful algae in California, USA. Harmful Algae 8 (1), 103–110.

Kudela, R.M., Seeyave, S., Cochlan, W.P., 2010. The role of nutrients in regulation and promotion of harmful algal blooms in upwelling systems. Prog. Oceanogr. 85, 122–135.

Kushnir, V.M., Tokarev, Y.N., Williams, R., Piontkovski, S.A., Evstigneev, P.V., 1997. Spatial heterogeneity of the bioluminescence field of the tropical Atlantic Ocean and its relationship with internal waves. Mar. Ecol. Prog. Ser. 160, 1–11.

Lapota, D., Geiger, M.L., Stiffey, A.V., Rosenberger, D.E., Young, D.K., 1989. Correlations of planktonic bioluminescence with other oceanographic parameters from a Norwegian Fjord. Mar. Ecol. Prog. Ser. 55, 217–227.

Lapota, D., Young, D.K., Bernstein, S.A., Geiger, M.L., Huddell, H.D., Case, J.S., 1992. Diel bioluminescence in heterotrophic and photosynthetic marine dinoflagellates in an Arctic fjord. J. Mar. Biol. Assoc. UK 72 (4), 733–744.

Latz, M.I., Jeong, H.J., 1996. Effect of red tide dinoflagellate diet on the bioluminescence of the heterotrophic dinoflagellate, *Protoperidinium* spp. Mar. Ecol. Prog. Ser. 132, 275–285.

Latz, M.I., Rohr, J., 2005. Glowing with the flow. Opt. Photon. News 16 (10), 40–45.

Le Quere, C., Harrison, S.P., Prentice, I.C., Buitenhuis, E.T., Aumont, O., et al., 2005. Ecosystem dynamics based on plankton functional types for global ocean biogeochemistry models. Glob. Chang. Biol. 11, 2016–2040.

Leterme, S.C., Edwards, M., Seuront, L., Attrill, M.J., Reid, P.C., John, A.W.G., 2005. Decadal basin-scale changes in diatoms, dinoflagellates, and phytoplankton color across the north Atlantic. Limnol. Oceanogr. 50 (4), 1244–1253.

Lewis, K., Allen, J.I., Richardson, A.J., Holt, J.T., 2006. Error quantification of a high resolution coupled hydrodynamic-ecosystem coastal-ocean model: part 3, validation with Continuous Plankton Recorder Data. J. Mar. Syst. 63, 209–224.

Limpert, E., Stahel, W.A., Abbt, M., 2001. Log-normal distributions across the sciences: keys and clues. Bioscience 51 (5), 341–352.

Litchman, E., Klausmeier, C.A., Schofield, O.M., Falkowski, P.G., 2007. The role of functional traits and trade-offs in structuring phytoplankton communities: scaling from cellular to ecosystem level. Ecol. Lett. 10, 1170–1181.

Lochte, K., Ducklow, H.W., Fasham, M.J.R., Stienen, C., 1993. Plankton succession and the carbon cycling at 47 N 20 W during the JGOFS North Atlantic bloom experiment. Deep-Sea Res. II 40, 91–114.

Losa, S., Kivman, G., Ryabchenko, V., 2004. Weak constraint parameter estimation for a simple ocean ecosystem model: what can we learn about the model and data? J. Mar. Syst. 45, 1–20.

Madec, G., 2008. NEMO ocean engine. Note du P^ole de mod'elisationInstitut Pierre-Simon Laplace (IPSL), France (No 27, ISSN No 1288–1619).

Marañón, E., Holligan, P.M., 1999. Photosynthetic parameters of phytoplankton from 50°N to 50°S in the Atlantic Ocean. Mar. Ecol. Prog. Ser. 176, 191–203.

Marcinko, C.L.J., Painter, S.C., Martin, A.P., Allen, J.T., 2013a. A review of the measurement and modelling of dinoflagellate bioluminescence. Prog. Oceanogr. 109, 117–129.

Marcinko, C.L.J., Allen, J.T., Poulton, A.J., Painter, S.C., Martin, A.P., 2013b. Diurnal variations of dinoflagellate bioluminescence within the open-ocean north-east Atlantic. J. Plankton Res. 35, 177–190.

Marra, J., 1995. Bioluminescence and optical variability in the ocean: an overview of the Marine Light-Mixed Layers Program. J. Geophys. Res. 100.

Menden-Deuer, S., Lessard, E.J., 2000. Carbon to volume relationships for dinoflagellates, diatoms and other protest plankton. Limnol. Oceanogr. 45 (3), 569–579.

Merico, A., Tyrrell, T., Lessard, E.J., Oguz, T., Stabeno, P.J., Zeeman, S.I., Whitledge, T.E., 2004. Modelling phytoplankton succession on the Bering Sea shelf: role of climate influences and trophic interactions in generating *Emiliania Huxleyi* blooms 1997–2000. Deep-Sea Res. I Oceanogr. Res. Pap. 51, 1803–1826.

Moline, M.A., Oliver, M.J., Mobley, C.D., Sundman, L., Bensky, T., Bergmann, T., Bissett, W.P., Case, J., Raymond, E.H., Schofield, O.M.E., 2007. Bioluminescence in a complex coastal environment: 1. temporal dynamics of nighttime water-leaving radiance. J. Geophys. Res. 112.

Montagnes, D.J.S., Chambouvet, A., Guillou, L., Fenton, A., 2008. Responsibility of microzooplankton and parasite pressure for the demise of toxic dinoflagellate blooms. Aquat. Microb. Ecol. 53, 211–225.

Neilson, D.J., Latz, M.I., Case, J.F., 1995. Temporal variability in the vertical structure of bioluminescence in the North Atlantic Ocean. J. Geophys. Res. 100.

Obayashi, Y., Tanoue, E., 2002. Growth and mortality rates of phytoplankton in the northwestern North Pacific estimated by the dilution method and HPLC pigment analysis. J. Exp. Mar. Biol. Ecol. 280, 33–52.

Odate, T., Imai, K., 2003. Seasonal variation in chlorophyll-specific growth and microzooplankton grazing of phytoplankton in Japanese coastal water. J. Plankton Res. 25 (12), 1497–1505.

Olascoaga, M.J., Beron-Vera, F.J., Brand, L.E., Koçak, H., 2008. Tracing the early development of harmful algal blooms on the West Florida Shelf with the aid of Lagrangian coherent structures. J. Geophys. Res. 113 (C12014).

Ondercin, D.G., Atkinson, C.A., Kiefer, D.A., 1995. The distribution of bioluminescence and chlorophyll during the late summer in the North-Atlantic—maps and a predictive model. J. Geophys. Res. Oceans 100, 6575–6590.

OSPAR Commission, 1998. Report of the modelling workshop on eutrophication issues. 5–8 November 1996. Den Haag, The Netherlands. OSPAR Report (86 pp.).

Petzoldt, T., Rudolf, L., Rinke, K., Benndorf, J., 2009. Effects of zooplankton diel vertical migration on a phytoplankton community: a scenario analysis of the underlying mechanisms. Ecol. Model. 220 (9–10), 1358–1368.

Popova, E.E., Srokosz, M.A., 2009. Modelling the ecosystem dynamics at the Iceland–Faeroes Front: biophysical interactions. J. Mar. Syst. 77, 182–196.

Qasim, S.Z., Bhattathiri, P.M.A., Devassy, V.P., 1973. Growth kinetics and nutrient requirements of two tropical marine phytoplankters. Mar. Biol. 21 (4), 299–304.

Radach, G., Moll, A., 2006. Review of three-dimensional ecological modelling related to the North Sea shelf system. Part II: model validation and data needs. Oceanogr. Mar. Biol. 44, 1–60 (An Annual Review).

Raitsos, D.E., Lavender, S.J., Maravelias, C.D., Haralabous, J., Richardson, A.J., Reid, P.C., 2008. Identifying four phytoplankton functional types from space: an ecological approach. Limnol. Oceanogr. 53 (2), 605–613.

Redfield, A.C., 1934. On the proportions of organic derivatives in sea water and their relation to the composition of plankton. In: Daniel, J.R. (Ed.), James Johnstone Memorial Volume. Liverpool University Press, pp. 176–192.

Richardson, A.J., Walne, A., John, A.W.G., Jonas, T., Lindley, J.A., Simms, D.W., Stevens, D., Witt, M., 2006. Using continuous plankton recorder data. Prog. Oceanogr. 68, 27–74.

Sarmiento, J.L., Slater, R.D., Fasham, M.J.R., Ducklow, H.W., Toggweiler, J.R., Evans, G.T., 1993. A seasonal three-dimensional ecosystem model of nitrogen cycling in the North Atlantic euphotic zone. Glob. Biogeochem. Cycles 7 (2), 417–450.

Sarthou, G., Timmermans, K.R., Blain, S., Tréguer, P., 2005. Growth physiology and fate of diatoms in the ocean: a review. J. Sea Res. 53 (1–2), 25–42.

Schartau, M., Oschlies, A., 2003. Simultaneous data-based optimization of a 1D-ecosystem model at three locations in the North Atlantic Ocean: part 1. Method and parameter estimates. J. Mar. Res. 61 (6), 765–793.

Seeyave, S., Probyn, T.A., Pitcher, G.C., Lucas, M.I., Purdie, D.A., 2009. Nitrogen nutrition in assemblages dominated by *Pseudo-nitzschia* spp., *Alexandrium catenella* and *Dinophysis acuminata* off the west coast of South Africa. Mar. Ecol. Prog. Ser. 379, 91–107.

Seliger, H.H., Fastie, W.G., Taylor, W.R., McElroy, W.D., 1962. Bioluminescence of marine dinoflagellates: i. an underwater photometer for day and night measurements. J. Gen. Physiol. 45, 1003–1017.

Shulman, I., Haddock, S.H.D., Mcgillicuddy, D.J., Paduan, J.D., Bissett, W.P., 2003. Numerical modeling of bioluminescence distributions in the coastal ocean. J. Atmos. Ocean. Technol. 20, 1060–1068.

Shulman, I., Moline, M.A., Penta, B., Anderson, S., Oliver, M., Haddock, S.H.D., 2011. Observed and modeled bio-optical, bioluminescent and physical properties during a coastal upwelling event in Monterey Bay, California. J. Geophys. Res. 116 (C01018).

Shulman, I., Penta, B., Moline, M.A., Haddock, S.H.D., Anderson, S., Oliver, M., Sakalaukus, P., 2012. Can vertical migrations of dinoflagellates explain observed bioluminescence patterns during an upwelling event in Monterey Bay, California? J. Geophys. Res. 117 (C1), C01016.

Sieracki, M.E., Verity, P.G., Stoecker, D.K., 1993. Plankton community response to sequential silicate and nitrate depletion during the 1989 North Atlantic spring bloom. Deep-Sea Res. II Top. Stud. Oceanogr. 40, 213–225.

Smayda, T.J., 1997. Harmful algal blooms: their ecophysiology and general relevance to phytoplankton blooms in the sea. Limnol. Oceanogr. 42, 1137–1153.

Smythe-Wright, D., Boswell, S.M., Kim, Y., Kemp, A.E., 2010. Spatio-temporal changes in the distribution of phytopigments and phytoplanktonic groups at the PAP. Deep-Sea Res. II 57 (15), 1324–1335.

Squire, J.L., Krumboltz, H., 1981. Profiling pelagic fish schools using airborne optical lasers and other remote sensing techniques. Mar. Technol. Soc. J. 15, 27–31.

Sullivan, J.M., Swift, E., 1995. Photoenhancement of bioluminescence capacity in natural and laboratory populations of the autotrophic dinoflagellate *Ceratium fusus* (Ehrenb.) Dujardin. J. Geophys. Res. 100 (C4), 6565–6574.

Sweeney, B.M., 1981. Variations in the bioluminescence per cell in dinoflagellates. In: Nealson, K.H. (Ed.), Bioluminescence Current Perspectives. Burgess Publishing, pp. 90–94.

Swift, E., Sullivan, J.M., Batchelder, H.P., Van Keuren, J., Vaillancourt, R.D., Bidigare, R.R., 1995. Bioluminescent organisms and bioluminescence measurements in the North Atlantic Ocean near latitude 59.5 °N, longitude 21 ° W. J. Geophys. Res.-Oceans 100.

Tang, E., 1996. Why do dinoflagellates have lower growth rates? J. Phycol. 32, 80–84.

Taylor, A.H., Harbour, D.S., Harris, R.P., Burkill, P.H., Edwards, E.S., 1993. Seasonal succession in the pelagic ecosystem of the North Atlantic and the utilization of nitrogen. J. Plankton Res. 15 (8), 875–891.

Tokarev, Y.N., Bityukov, E.P., Williams, R., Vasilenko, V.I., Piontkovski, S.A., Sokolov, B.G., 1999. The bioluminescence field as an indicator of the spatial structure and physiological state of the planktonic community at the Mediterranean sea basin. In: Malanotte-Rizzoli, P., Eremeev, V.N. (Eds.), The Eastern Mediterranean as a Laboratory Basin for the Assessment of Contrasting Ecosystems. The Netherlands, pp. 407–416.

Vanhoutte-Brunier, A., Fernand, L., Ménesguen, A., Lyons, S., Gohin, F., Cugier, P., 2008. Modelling the *Karenia mikimotoi* bloom that occurred in the western English Channel during summer 2003. Ecol. Model. 210, 351–376.

Verity, P.G., Stoecker, D.K., Sieracki, M.E., Nelson, J.R., 1993. Grazing and the mortality of microzooplankton during the 1989 North Atlantic spring bloom at 47 N 18 W. Deep-Sea Res. II 40 (9), 1793–1814.

Vichi, M., Pinardi, N., Masina, S., 2007. A generalized model of pelagic biogeochemistry for the global ocean ecosystem. Part I: theory. J. Mar. Syst. 64, 89–109.

Walsh, J.J., Penta, B., Dieterle, D.A., Bissett, W.P., 2001. Predictive ecological modeling of harmful algal blooms. Crc Press Llc, Research Triangle Pk, Nc, pp. 1369–1383.

Ward, B.A., Schartau, M., Oschlies, A., Martin, A.P., Follows, M.J., Anderson, T.R., 2013. When is a biogeochemical model too complex? Objective model reduction and selection for North Atlantic time-series sites. Prog. Oceanogr. 116, 49–65.

Widder, E.A., 2010. Bioluminescence in the ocean: origins of biological, chemical and ecological diversity. Science 328, 704.